Pergamon

Int. J. Solids Structures Vol. 32, No. 22, pp. 3289–3305, 1995

0020–7683/95 $9.50 + .00

0020-7683(94)00310-6

TOUGHENING DUE TO TRANSFORMATIONS INDUCED BY A CRACK TIP STRESS FIELD IN FERROELASTIC MATERIALS

C. Q. RU
Department of Mechanical Engineering, University of Alberta, Edmonton, Alberta T6G 2G8, Canada

and

R. C. BATRA
Department of Engineering Science and Mechanics, Virginia Polytechnic Institute and State University, Blacksburg, VA 24061-0219 U.S.A.

(*Received* 8 *August* 1994; *in revised form* 21 *November* 1994)

Abstract—We examined the effects on the SIF (stress intensity factor) of the deviatoric and shear ferroelastic transformations and phase switching near the crack tip for plane strain deformations of ferroelastic-type crystals. Motivated by experimental observations, we confined ourselves to those materials whose paraelastic phase is marked by low anisotropy and therefore can be idealized as isotropic. It was found that the transformed zone ahead of a stationary crack tip contributes nothing to the SIF for single and bi-crystals. However, the transformed wake left behind the steadily growing quasi-static crack tip always reduced the SIF considerably; this toughening effect is very sensitive to the mismatch angles between the crack surface and the principal axes of the transformed material for ferroelastic switching, but not for ferroelastic transformations. The numerical results for the steady-state and quasi-static crack growth were verified by the energy method. The computed results agree qualitatively with the observed values for NiTi-SMA of low anisotropy.

1. INTRODUCTION

Transformation toughening has long been known for the TRIP (TRansformation-Induced Plasticity) steels (Gerberich *et al.*, 1969; Antolovich and Singh, 1971). However, there has been a surge of interest [e.g. see Evans (1989) and Green *et al.* (1989)] in this field since Garvie *et al.* (1975) discovered that the martensitic transformation triggered by the elevated crack tip stress will considerably reduce the SIFs (stress intensity factors) and therefore enhance the fracture toughness for zirconia-reinforced ceramic systems. Such a toughening phenomenon has been explained successfully by examining the interaction between the deformation field and the transformation-induced strain near the crack tip. The related transformation has been modeled as pure dilatant by McMeeking and Evans (1982) and Budiansky *et al.* (1983), and the effects of shear stresses and shear strains on transformation toughening have been examined by, among others, Lambropoulos (1986), Stump (1989), Karihaloo and Huang (1989) and Budiansky and Truskinovsky (1993).

The similar problem for ferroelectric and other materials in which the stress-induced phase transformation plays an indispensable role in their fracture behavior is also of interest. We note that the effects of transformation on fracture behavior in ferroelectric materials (e.g. $BaTiO_3$) have been examined [e.g. see Pohanka *et al.* (1978) and Freiman (1986)]. It is found that the fracture toughness in the ferroelectric state is considerably higher than that in the paraelectric state, and such a toughening phenomenon has been attributed to the interaction between the crack tip and the ferroelectric domain wall formed during the paraelectric → ferroelectric phase transformation. The paraelectric → ferroelectric phase transformation is basically temperature-induced, even though the pressure may affect the temperature (Fatuzzo and Merz, 1967) at which the transformation occurs. The mechanical analogy of a ferroelectric material is a ferroelastic material, i.e. a material which exhibits two or more stable states characterized by different spontaneous strain in the absence of external mechanical loads; the material in one state can be transformed into

another state by applying mechanical loads (Aizu, 1969). Therefore, it is of interest to examine the effects of phase transformations on the fracture behavior of ferroelastic materials.

Even though the transformation strain for some ferroelastic materials is large, we use the kinematically linear theory here. Within the framework of a linear theory, the strain can be divided into the dilatational, deviatoric and shear components, and therefore the two basic kinds of transformations in ferroelastic materials are the deviatoric and shear transformations. The constitutive theory of deviatoric transformations has been developed by, among others, Barsch and Krumhansl (1988) and Jacobs (1985, 1992), and that of shear transformations may be developed in the same way. Henceforth, for brevity, we call deviatoric and shear transformations in ferroelastic materials ferroelastic deviatoric and ferroelastic shear transformations. We note that the mechanical behavior of a SMA (shape memory alloy) under a certain range of low temperatures has been modeled by the ferroelastic-type shear transformation by Falk (1980) and Achenbach and Muller (1985). Several other related references may be found in the proceedings of a conference edited by Delaey and Chandrasekaran (1982).

Here, we examine the effects on the SIF of deviatoric and shear transformations and ferroelastic switching induced by the crack tip stress field for plane strain deformations of ferroelastic crystals. We confine ourselves to those materials whose paraelastic (parent) phases are marked by low anisotropy and therefore regard them as isotropic. This assumption is motivated by experiments on NiTi-SMAs for which it has been found (Melton and Mercier, 1981; Miyazaki *et al.*, 1982; Mukunthan and Brown, 1988) that their higher fracture toughness is attributable to the lower anisotropy of their parent phases. We note that the copper-based SMA has a poor fracture behavior in the bi-crystal state due to the mismatch of the transformation strain at the interface created by large anisotropy.

It is found that the stationary transformed zone has a null contribution to the SIF for both phase transformations and ferroelastic switching. However, the transformed wake left behind the steadily growing quasi-static crack tip noticeably reduces the SIF; this toughening effect is sensitive to the mismatch angles between the crack surface and the principal axes of the transformed material for ferroelastic switching, but not for ferroelastic transformations. Numerical results for the steady-state crack growth are verified by the energy method. These results are in qualitative agreement with the experimental observations for NiTi-SMAs of low anisotropy.

2. CONSTITUTIVE RELATIONS FOR A FERROELASTIC MATERIAL

For plane strain deformations of a linear isotropic material, the strain energy density per unit volume can be written as

$$W(\varepsilon_{11}, \varepsilon_{12}, \varepsilon_{22}) = A\eta_1^2 + B\eta_2^2 + D\eta_3^2, \tag{1}$$

where $A = \mu/[2(1-2\nu)]$, $B = \mu/2$ and $D = 2\mu$, μ and ν are, respectively, the shear modulus and Poisson's ratio, $\varepsilon_{\alpha\beta}$ the strain components for infinitesimal deformations of the body with respect to a set of rectangular Cartesian axes, and η_1, η_2 and η_3 their dilatational, deviatoric and shear combinations, respectively. That is,

$$\eta_1 = \varepsilon_{11} + \varepsilon_{22}, \quad \eta_2 = \varepsilon_{11} - \varepsilon_{22}, \quad \eta_3 = \varepsilon_{12}. \tag{2}$$

A continuum theory, based on the free-energy function $W(\varepsilon_{11}, \varepsilon_{12}, \varepsilon_{22})$, to describe the deviatoric transformations under plane strain deformations of ferroelastic crystals has been developed by, among others, Barsch and Krumhansl (1988) and Jacobs (1985, 1992):

$$W(\varepsilon_{11}, \varepsilon_{12}, \varepsilon_{22}) = F(\eta_2) + A\eta_1^2 + D\eta_3^2, \quad A > 0, D > 0, \tag{3}$$

where A and D are two independent positive material constants, and $F(\eta_2)$ is assumed to be a Landau-type function,

$$F(\eta_2) = F_2\eta_2^2 - F_4\eta_2^4 + F_6\eta_2^6, \quad F_2 > 0, F_4 > 0, F_6 > 0,$$

where all strain gradient terms in the expression for the strain energy density employed by Barsch and Krumhansl (1988) and Jacobs (1985, 1992) used to describe the structure of the interface have been omitted. The constitutive relation (3) has been used to describe the phase transformations in materials such as Nb_3Sn, V_3Si and In–Tl alloys (Barsch and Krumhansl, 1988; Jacobs, 1985, 1992). The material described by eqn (3) is anisotropic.

We note that piecewise linearized constitutive relations have often been adopted for ferroelastic and ferroelectric materials, e.g. see the so-called "square-hysteretic" constitutive curve in Aizu (1969) and Fatuzzo and Merz (1967). Several previous works on transformation toughening have presumed a trilinear stress–strain constitutive relation with two distinct stable phases having the same modulus (McMeeking and Evans, 1982; Budiansky *et al.*, 1983). Here, we adopt a piecewise linearized relation for $f(\cdot) \equiv F'(\cdot)$, as shown in Fig. 1, where the slopes of the two stable branches are taken to be equal to each other.

The ferroelastic-type shear transformation has also been adopted as a simplified model for phase transformations in some SMAs by Falk (1980) and Achenbach and Muller (1985). Therefore, when studying the shear ferroelastic transformation, we assume the strain energy density to be given by

$$W(\varepsilon_{11}, \varepsilon_{12}, \varepsilon_{22}) = G(\eta_3) + A\eta_1^2 + B\eta_2^2, \quad A > 0, B > 0, \tag{4}$$

where $g(\cdot) \equiv G'(\cdot)$ is a piecewise linearized function shown in Fig. 1. A similar assumption has been made by Falk (1980) and Achenbach and Muller (1985) for studying one-dimensional deformations of SMAs at low temperatures.

For the strain energy density (3), expressions for stress components are

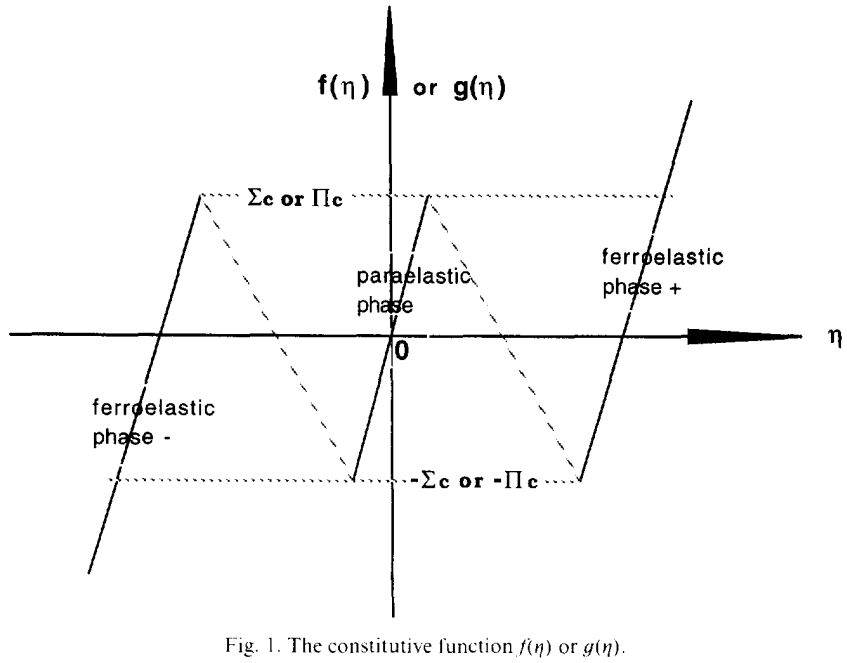

Fig. 1. The constitutive function $f(\eta)$ or $g(\eta)$.

$$\sigma_{11} = \partial W/\partial \varepsilon_{11} = f(\varepsilon_{11}-\varepsilon_{22})+2A(\varepsilon_{11}+\varepsilon_{22})$$
$$\sigma_{12} = (1/2)\,\partial W/\partial \varepsilon_{12} = B\varepsilon_{12}$$
$$\sigma_{22} = \partial W/\partial \varepsilon_{22} = -f(\varepsilon_{11}-\varepsilon_{22})+2A(\varepsilon_{11}+\varepsilon_{22}). \tag{5}$$

For the material initially in the paraelastic phase, we assume that when $(\sigma_{11}-\sigma_{22})$ reaches a critical value Σ_c (or $-\Sigma_c$), the material undergoes a phase transformation from the paraelastic phase to one of two ferroelastic phases and η_2 jumps by 2δ. For the transformation to the "Σ_+ phase", the transformation strain $\varepsilon^*_{x\beta}$ assumes the values

$$\varepsilon^*_{11} = \delta, \quad \varepsilon^*_{12} = \varepsilon^*_{21} = 0, \quad \varepsilon^*_{22} = -\delta, \tag{6}$$

and for the transformation to the "Σ_- phase", η_2 jumps by -2δ, and

$$\varepsilon^*_{11} = -\delta, \quad \varepsilon^*_{12} = \varepsilon^*_{21} = 0, \quad \varepsilon^*_{22} = \delta, \tag{7}$$

where δ is a constant associated with the deviatoric transformation and typically equals 0.1–0.15 (Jacobs, 1985, 1992). This transformation from the paraelastic phase to one of two ferroelastic phases is irreversible, even though the transformation between two ferroelastic phases is reversible. The stress-induced transformation between two ferroelastic phases is referred to as "ferroelastic switching"; the switching-related toughening phenomenon will be discussed in Section 6.

We assume that the paraelastic (parent) phase described by eqn (3) can be approximated as isotropic so that three constants A, D and B^*, where B^* is the constant modulus for the piecewise linearized curve f vs η_2 shown in Fig. 1, are related to the shear modulus μ and Poisson's ratio ν by

$$B^* = \mu/2, \quad A = \mu/[2(1-2\nu)], \quad D = 2\mu. \tag{8}$$

The conditions for the isotropy of the paraelastic phase with three material constants (A, B^* and D) are

$$D = 4B^*, \quad A \geqslant B^*, \tag{9}$$

which are satisfied by eqn (8). Since the moduli of three phases for a trilinear material are equal to each other, the isotropy of the paraelastic phase implies the isotropy of the mechanical response of the two ferroelastic phases.

Similarly, for the strain energy density (4), the stresses are given by

$$\sigma_{11} = \partial W/\partial \varepsilon_{11} = 2A\eta_1 + 2B\eta_2$$
$$\sigma_{12} = (1/2)\partial W/\partial \varepsilon_{12} = g(\eta_3)/2$$
$$\sigma_{22} = \partial W/\partial \varepsilon_{22} = 2A\eta_1 - 2B\eta_2. \tag{10}$$

For the material initially in the paraelastic phase, we assume that when σ_{12} reaches a critical value Π_c (or $-\Pi_c$), the material undergoes a shear transformation from the paraelastic phase to one of two ferroelastic phases, and η_3 jumps by the phase transformation constant ε (cf. Fig. 1). For the transformation to the "Π_+ phase", η_3 jumps by ε and the transformation strains are given by

$$\varepsilon^*_{11} = 0, \quad \varepsilon^*_{12} = \varepsilon^*_{21} = \varepsilon, \quad \varepsilon^*_{22} = 0; \tag{11}$$

for the transformation to the "Π_- phase", η_3 jumps by $-\varepsilon$ and the transformation strains are

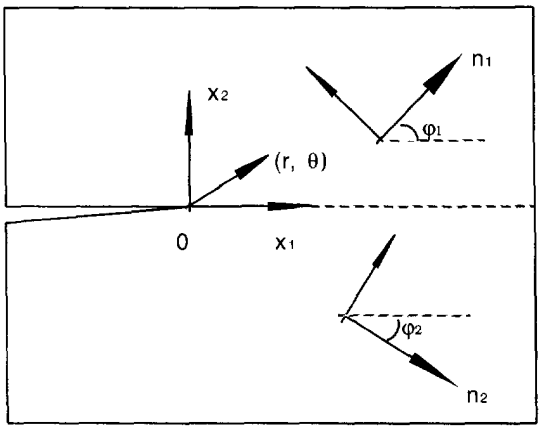

Fig. 2. A semi-infinite crack in the ferroelastic bi-crystal.

$$\varepsilon_{11}^{*} = 0, \quad \varepsilon_{12}^{*} = \varepsilon_{21}^{*} = -\varepsilon, \quad \varepsilon_{22}^{*} = 0. \tag{12}$$

We assume that the function $g(\eta_3)$ can be modeled by a "trilinear curve", with the constant modulus D^*, as shown in Fig. 1, and the paraelastic phase can be approximated as isotropic, for which three constants A, B and D^* are related to μ and ν by eqn (8), with B and D^* replacing B^* and D, respectively. The transformation between two distinct ferroelastic phases is referred to as "ferroelastic switching" and will be discussed in Section 6.

We consider the general case when at least one of the principal axes $\{n, t\}$ of the transformed material is not necessarily parallel (or perpendicular) to the x_1-axis (see Fig. 2). For this case, it is readily seen that all of the above formulae are valid provided that we replace $\{x_1, x_2\}$ by $\{n, t\}$.

3. FORMULATION FOR TRANSFORMATION TOUGHENING

We study the toughening effects of stress-induced transformations in ferroelastic materials described by constitutive relations (3) and (4).

Consider a semi-infinite crack along the bi-crystal interface $x_2 = 0$ and occupying the domain $x_1 < 0$, the upper and lower half-planes are made of the same material with the same material constants; however, the orientations of principal axes of the transformed material in the upper and lower half planes, expressed by φ_1 and φ_2 respectively and shown in Fig. 2, are arbitrary and different in general. A single crystal is a special case for which the upper and lower half-planes have the same orientation, thus $\varphi_1 + \varphi_2 = \pi/2$.

When no transformation takes place, the interface disappears due to the identity of two half-planes. Therefore, the transformation-free stress field is given by the classical elastic stress field of mode I. McMeeking and Evans (1982) and Green *et al.* (1989), among others, have shown that the transformation region can be estimated satisfactorily by the transformation-free stress field for dilatational transformations when the transformed zone is small. We adopt this simplification here. In other words, we neglect the influence on the size of the transformation zone of the additional stress field induced by the transformation strain. This simplifies the analysis; however, the so-called "lock-up" phenomenon cannot be studied. The transformed zone and the contribution ΔK_I to the SIF and hence to the toughening in the upper and lower half-planes can be calculated separately. Since ΔK_I is additive for the upper and lower half-planes, without loss of generality, we confine our discussion to the upper half-plane; the result will also be applicable to the lower half-plane.

If we denote the mode I SIF of the virgin material by K_I^0, and the additional SIF induced by the transformation by ΔK_I, then the total SIF, K_I, is given by

$$K_1 = K_1^0 + \Delta K_1. \tag{13}$$

We use the polar coordinate system $\{r, \theta\} : r \geqslant 0, \pi \geqslant \theta \geqslant -\pi$. As shown in Fig. 2, let the angle between a principal axis of the material in the upper half-plane and the x_1-direction be $\varphi_1 = \varphi$, $0 \leqslant \varphi \leqslant \pi/2$. For any point $\{r, \theta\}$, the deviatoric and shear stress components with respect to the principal axes $\{n, t\}$ of the transformed material are given in terms of $\{\sigma_{11}, \sigma_{22}, \sigma_{12}\}$ by

$$\begin{aligned}(\sigma_{nn} - \sigma_{tt}) &= (\sigma_{11} - \sigma_{22}) \cos 2\varphi + 2\sigma_{12} \sin 2\varphi \\ \tau_{nt} &= (\sigma_{22} - \sigma_{11}) \cos \varphi \sin \varphi + \sigma_{12} \cos 2\varphi.\end{aligned} \tag{14}$$

Since the paraelastic phase is isotropic and the transformed zone is determined by the transformation-free stress fields, we substitute the classical elastic stress field of mode I into eqns (14) and obtain

$$(\sigma_{nn} - \sigma_{tt}) = [K_1^0 \sqrt{(2\pi r)}] \sin \theta \sin (2\varphi - 1.5\theta) \tag{15}$$

$$\tau_{nt} = [K_1^0 \sqrt{(8\pi r)}] \sin \theta \cos (2\varphi - 1.5\theta). \tag{16}$$

Because of the appearance of $\sin \theta$ in eqns (15) and (16), the radius of the transformed zone will vanish along the interface $\theta = 0$. Thus, there is no transformation strain incompatibility at the interface: this is true only for isotropic bi-crystals and may be approximately valid for materials of low anisotropy. For bi-crystals of large anisotropy (Melton and Mercier, 1981; Miyazaki *et al.*, 1982), the incompatibility of the transformation strain at the interface will lead to an additional SIF which will increase the local stress concentration. This is why a bi-crystal of large anisotropy exhibits poor resistance to intergranular fracture.

When $(\sigma_{nn} - \sigma_{tt})$ reaches the critical value Σ_c at a point, as stated in the previous section, the material element at that point will undergo a deviatoric transformation: $\varepsilon_{nn} = \delta$, $\varepsilon_{tt} = -\delta$ and $\varepsilon_{nt} = \varepsilon_{tn} = 0$. Similarly, if τ_{nt} reaches the critical value Π_c at a point, then the material element there will undergo a shear transformation: $\varepsilon_{nn} = 0$, $\varepsilon_{tt} = 0$ and $\varepsilon_{nt} = \varepsilon_{tn} = \varepsilon$. Once the transformation occurs, the transformation strains in the $\{x_1, x_2\}$ frame are given by

$$\varepsilon_{12} = \varepsilon_{21} = \delta \sin 2\varphi, \quad \varepsilon_{11} = \delta \cos 2\varphi, \quad \varepsilon_{22} = -\varepsilon_{11} = -\delta \cos 2\varphi \tag{17}$$

for the deviatoric case, and

$$\varepsilon_{12} = \varepsilon_{21} = \varepsilon \cos 2\varphi, \quad \varepsilon_{11} = -\varepsilon \sin 2\varphi, \quad \varepsilon_{22} = -\varepsilon_{11} = \varepsilon \sin 2\varphi \tag{18}$$

for the shear case. For the inverse deviatoric and shear transformations, formulae (17) and (18) are valid with δ and ε replaced by $-\delta$ and $-\varepsilon$, respectively.

The SIF induced by the transformation strains $\varepsilon^*_{\alpha\beta}$ is calculated by using the formulae given in Hutchinson (1974) and Gao (1989), with the following results:

$$\Delta K_1^{22} = \frac{2\mu C}{8} \varepsilon^*_{22} \int_\Omega [7 \cos (3\theta/2) - 3 \cos (7\theta/2)] r^{-1/2} \, d\theta \, dr$$

$$\Delta K_1^{11} = \frac{2\mu C}{8} \varepsilon^*_{11} \int_\Omega [7 \cos (3\theta/2) + 3 \cos (7\theta/2)] r^{-1/2} \, d\theta \, dr$$

$$\Delta K_1^{12} = \frac{3\mu C}{4} \varepsilon^*_{12} \int_\Omega [\sin (7\theta/2) - \sin (3\theta/2)] r^{-1/2} \, d\theta \, dr,$$

$$\Delta K_{\mathrm{I}} = \Delta K_{\mathrm{I}}^{11} + \Delta K_{\mathrm{I}}^{22} + 2\Delta K_{\mathrm{I}}^{12}, \tag{19}$$

where μ is the shear modulus, $C = 1/[2(1-\nu)(2\pi)^{1/2}]$, and Ω is the transformed region.

Substituting eqns (17) and (18) into eqns (19), the SIFs induced by the deviatoric and shear transformations are given by

$$\Delta K_{\mathrm{I}} = \pm 3\mu\delta C \int_{\Omega} \sin(\theta) \sin(2\varphi - 5\theta/2) r^{-1/2}\, \mathrm{d}\theta\, \mathrm{d}r \tag{20}$$

$$\Delta K_{\mathrm{I}} = \pm 3\mu\varepsilon C \int_{\Omega} \sin(\theta) \cos(2\varphi - 5\theta/2) r^{-1/2}\, \mathrm{d}\theta\, \mathrm{d}r, \tag{21}$$

respectively. The sign "+" is taken for transformed regions with "Σ_+ or Π_+ phase" and "−" is taken for transformed regions with "Σ_- or Π_- phase", respectively.

We note that the size Ω of the transformed zone depends on the crack growth condition; here we consider the steady-state and quasi-static crack growth. The transformed zone is divided into two parts, the transformed loading zone (Budiansky *et al.*, 1983) ahead of the crack tip and the transformed unloading wake behind the advancing crack tip. Therefore, we divide ΔK_{I} into two parts:

$$\Delta K_{\mathrm{I}} = \Delta K_{\mathrm{I}}(S) + \Delta K_{\mathrm{I}}(W), \tag{22}$$

where $\Delta K_{\mathrm{I}}(S)$ and $\Delta K_{\mathrm{I}}(W)$ denote contributions to the SIF from the transformed loading zone and the transformed unloading wake, respectively. $\Delta K_{\mathrm{I}}(S)$ is found to equal the SIF induced by the stationary transformed zone. We evaluate $\Delta K_{\mathrm{I}}(S)$ first for a stationary crack.

4. STATIONARY CRACK

Budiansky *et al.* (1983) have shown that for the dilatational transformation, the stationary transformed zone contributes nothing to the SIF. We show below that the same is true for the ferroelastic transformation studied herein.

4.1. *Deviatoric transformations*

Using eqn (15), the radius $r^*(\theta)$ of the stationary transformed zone is given by

$$r^*(\theta) = (1/2\pi)[K_{\mathrm{I}}^0/\Sigma_c]^2 [\sin\theta \sin(2\varphi - 1.5\theta)]^2, \quad \text{or } x_2^*(\theta) = \sin\theta r^*(\theta). \tag{23}$$

Thus, for a half-plane

$$\frac{\Delta K_{\mathrm{I}}^{(S)}}{\alpha K_{\mathrm{I}}^0} = 3\sqrt{2} \int_0^{\pi} \sin^2(\theta) \sin(2\varphi - 2.5\theta) \sin(2\varphi - 1.5\theta)\, \mathrm{d}\theta, \tag{24}$$

where

$$\alpha = \frac{\mu\delta C}{\sqrt{\pi}\Sigma_c} \tag{25}$$

is a nondimensional number. Noting that

$$\int_0^{\pi} \sin^2(\theta)\cos(\theta)\,\mathrm{d}\theta = 0, \quad \int_0^{\pi} \sin^2(\theta)\cos(4\theta)\,\mathrm{d}\theta = 0, \quad \int_0^{\pi} \sin^2(\theta)\sin(4\theta)\,\mathrm{d}\theta = 0, \tag{26a}$$

we obtain

$$\Delta K_{\mathrm{I}}^{(S)} = 0. \tag{26b}$$

Therefore, the contribution of the stationary transformed zone to the SIF is always null.

4.2. *Shear transformations*

Using eqn (16), the radius $r^*(\theta)$ of the stationary transformed zone for the shear transformation is given by

$$r^*(\theta) = (1/8\pi)[K_{\mathrm{I}}^0/\Pi_c]^2[\sin\theta\cos(2\varphi - 1.5\theta)]^2 \tag{27}$$

and for a half-plane

$$\frac{\Delta K_{\mathrm{I}}^{(S)}}{\beta K_{\mathrm{I}}^0} = \frac{3}{\sqrt{2}}\int_0^{\pi} \sin^2(\theta)\cos(2\varphi - 2.5\theta)\cos(2\varphi - 1.5\theta)\,\mathrm{d}\theta, \tag{28}$$

where

$$\beta = \frac{\mu\varepsilon C}{\Pi_c\sqrt{\pi}} \tag{29}$$

is a nondimensional number. Using eqn (26a), we conclude that

$$\Delta K_{\mathrm{I}}^{(S)} = 0. \tag{30}$$

Thus, the contribution of the stationary transformed zone to the SIF is zero.

5. STEADY-STATE AND QUASI-STATIC CRACK GROWTH

As far as toughening is concerned, the transformed loading zone is equivalent to the stationary transformed zone, whose effect has been found to be null. Therefore, we find the contribution to toughening of the transformed unloading wake behind the steadily growing crack tip.

5.1. *Deviatoric transformations*

The size of the transformed wake in deviatoric transformations depends strongly on the angle φ between the material principal axis and the x_1-axis. Values of variables determining the size of the transformed wake for nine values of the angle φ are given in Table

Table 1. Values of variables for the deviatoric ferroelastic transformation in a half-plane

φ	$H^*/[(K_I^0/\Sigma_c)^2\pi]$	θ^*	$H^{**}/[(K_I^0/\Sigma_c)^2\pi]$	θ^{**}	$\Delta K_I/[\alpha K_I^0]$	Others
0	0.035	2.5	0.38	1.25	−1.27	$\theta_0 \approx 2.09$
$\pi/16$	0.01	2.7	0.47	1.4	−1.38	$\theta_0 \approx 2.35$
$\pi/8$	<0.0015	2.8 and 0.3	0.5	1.57	−1.42	$\theta_0 \approx 2.61$
$3\pi/16$	0.01	0.45	0.47	1.7	−1.38	$\theta_0 \approx 0.78$; $\underline{\theta}^* \approx 0.9$
$\pi/4$	0.035	0.6	0.39	1.9	−1.29	$\theta_0 \approx 1.05$; $\underline{\theta}^* \approx 1.2$
$5\pi/16$	0.085	0.75	0.27	2.0	−1.24	$\theta_0 \approx 1.31$; $\underline{\theta}^* \approx 1.6$
$3\pi/8$	0.17	0.9	0.17	2.2	−1.44	$\theta_0 \approx 1.57$
$7\pi/16$	0.28	1.1	0.08	2.35	−1.24	$\theta_0 \approx 1.83$
$\pi/2$	0.38	1.25	0.035	2.5	−1.27	$\theta_0 \approx 2.09$

1, where H^* denotes the height of the "+ phase" transformed wake in the upper half-plane and θ^* the corresponding angle at which H^* is realized; similarly, H^{**} equals the height of the "− phase" transformed wake and θ^{**} the corresponding angle at which H^{**} is realized. According to the condition $(\sigma_{nn}-\sigma_{rr}) = \pm\Sigma$, there will be three transformed regions over a half-plane for some values of the angle φ; however, it is found that the height of one of them is always very small as compared to those of the other two and is therefore omitted from subsequent discussion. The two noticeably transformed regions are shown in Figs 3 and 4.

The discussion below is divided into three cases according to the range of φ; the corresponding values of H^*, H^{**}, θ^* and θ^{**} are given in Table 1.

Case (a). $0 \leqslant \varphi \leqslant \pi/8$. We have

$$H^{**} > H^* \quad \text{but} \quad \theta^* > \theta^{**}.$$

The transformed wake has the shape shown in Fig. 3(a) and we have the following expression for the induced SIF for a half-plane:

$$\frac{\Delta K_I}{\alpha K_I^0} = -6\int_{\theta^{**}}^{\theta^*} \sin(\theta)\sin(2\varphi-2.5\theta)\left(\frac{\sqrt{H^{**}}}{\sqrt{\sin(\theta)}} - \frac{\sin(\theta)|\sin(2\varphi-1.5\theta)|}{\sqrt{2}}\right)d\theta$$
$$-6\int_{\theta^*}^{\pi} \sin(\theta)\sin(2\varphi-2.5\theta)\left(\frac{\sqrt{H^{**}}}{\sqrt{\sin(\theta)}} - 2\frac{\sqrt{H^*}}{\sqrt{\sin(\theta)}} + \frac{\sin(\theta)|\sin(2\varphi-1.5\theta)|}{\sqrt{2}}\right)d\theta. \quad (31)$$

Case (b). $\pi/8 < \varphi < 3\pi/8$. From Fig. 3(b), we have

$$H^{**} > H^* \quad \text{with} \quad \theta^{**} > \theta^*.$$

Therefore, the induced SIF for a half-plane is given by

$$\frac{\Delta K_I}{\alpha K_I^0} = -6\int_{\theta^{**}}^{\pi} \sin(\theta)\sin(2\varphi-2.5\theta)\left(\frac{\sqrt{H^{**}}}{\sqrt{\sin(\theta)}} - \frac{\sin(\theta)|\sin(2\varphi-1.5\theta)|}{\sqrt{2}}\right)d\theta$$
$$+6\int_{\theta^*}^{\theta^*} \sin(\theta)\sin(2\varphi-2.5\theta)\left(\frac{\sqrt{H^*}}{\sqrt{\sin(\theta)}} - \frac{\sin(\theta)|\sin(2\varphi-1.5\theta)|}{\sqrt{2}}\right)d\theta, \quad (32)$$

where angle $\underline{\theta}^*$ is shown in Fig. 3(b).

Case (c). $3\pi/8 \leqslant \varphi \leqslant \pi/2$. We now have

$$H^{**} \leqslant H^* \quad \text{with} \quad \theta^{**} > \theta^*$$

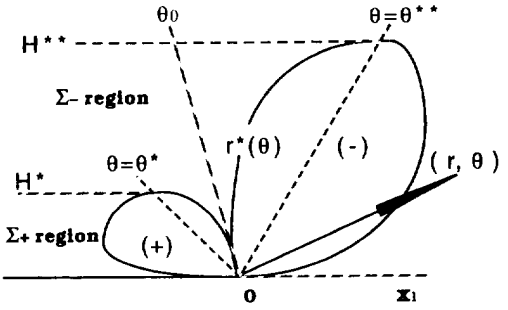

a). $0 \leq \varphi \leq \pi/8$

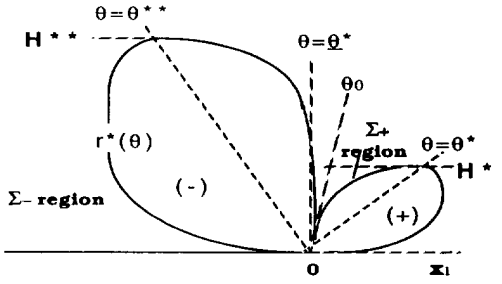

b). $\pi/8 < \varphi < 3\pi/8$

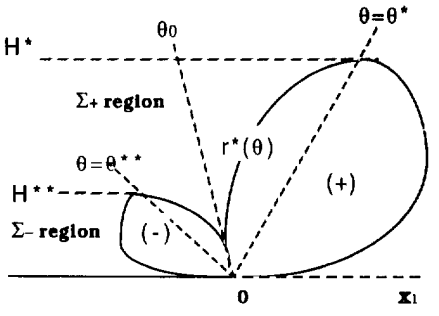

c). $3\pi/8 \leq \varphi \leq \pi/2$

Fig. 3. Transformation zones, due to deviatoric transformations, for steady-state and quasi-static crack growth in a half-plane. (a) $0 \leqslant \varphi \leqslant \pi/8$; (b) $\pi/8 < \varphi < 3\pi/8$; (c) $3\pi/8 \leqslant \varphi \leqslant \pi/2$.

and obtain the following expression for the induced SIF for a half-plane:

$$\frac{\Delta K_{\mathrm{I}}}{\alpha K_{\mathrm{I}}^{0}} = 6\int_{\theta^{*}}^{\theta^{**}} \sin(\theta)\sin(2\varphi-2.5\theta)\left(\frac{\sqrt{H^{*}}}{\sqrt{\sin(\theta)}} - \frac{\sin(\theta)|\sin(2\varphi-1.5\theta)|}{\sqrt{2}}\right)\mathrm{d}\theta\,\mathrm{d}r$$

$$+6\int_{\theta^{**}}^{\pi} \sin(\theta)\sin(2\varphi-2.5\theta)\left(\sqrt{\frac{H^{*}}{\sin(\theta)}} - 2\sqrt{\frac{H^{**}}{\sin(\theta)}} + \frac{\sin(\theta)|\sin(2\varphi-1.5\theta)|}{\sqrt{2}}\right)\mathrm{d}\theta\,\mathrm{d}r. \quad (33)$$

5.2. *Shear transformations*

For the shear transformations, the data for the transformed wake for nine values of angle φ is given in Table 2. We shall use H^{*}, H^{**}, θ^{*} and θ^{**} in the same sense as that in Section 5.1 and give below the characteristics of the transformed wake according to the range of φ; the corresponding values of H^{*}, H^{**}, θ^{*}, $\underline{\theta^{*}}$ and θ^{**} are given in Table 2.

Case (a). $0 \leqslant \varphi \leqslant \pi/8$. From Fig. 4(a), it follows that

$$H^{*} \leqslant H^{**} \text{ with } \theta^{*} < \theta^{**}.$$

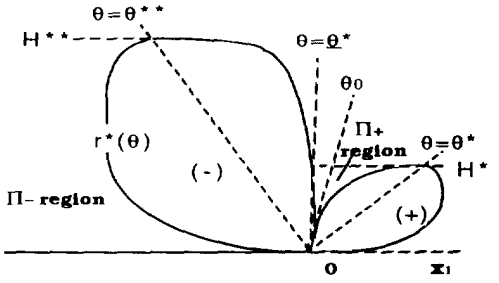

a). $0 \le \varphi \le \pi/8$

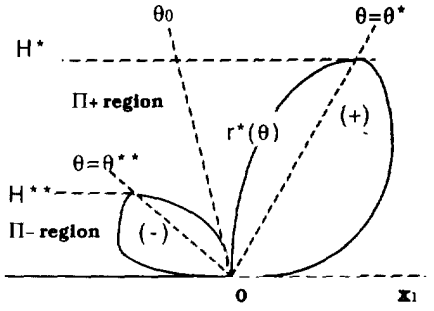

b). $\pi/8 < \varphi < 3\pi/8$

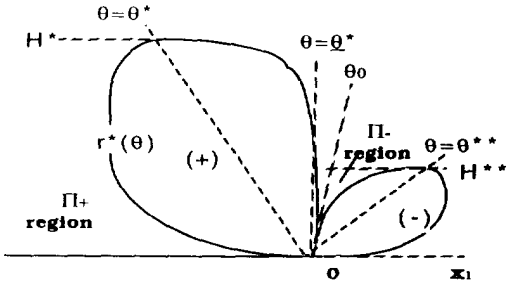

c). $3\pi/8 \le \varphi \le \pi/2$

Fig. 4. Transformation zones, due to shear transformations, for steady-state and quasi-static crack growth in a half-plane. (a) $0 \leqslant \varphi \leqslant \pi/8$; (b) $\pi/8 < \varphi < 3\pi/8$; (c) $3\pi/8 \leqslant \varphi \leqslant \pi/2$.

Table 2. Values of variables for the shear ferroelastic transformation in a half-plane

φ	$H^*/[(K_I^0/\Pi_c)^2/\pi]$	θ^*	$H^{**}/[(K_I^0/\Pi_c)^2/\pi]$	θ^{**}	$\Delta K_I/[\beta K_I^0]$	Others
0	0.0085	0.60	0.097	1.86	−0.64	$\theta_0 \approx 1.05$; $\underline{\theta}^* \approx 1.2$
$\pi/16$	0.02	0.75	0.070	2.0	−0.63	$\theta_0 \approx 1.31$; $\underline{\theta}^* \approx 1.60$
$\pi/8$	0.045	0.92	0.045	2.2	−0.75	$\theta_0 \approx 1.57$; $\underline{\theta}^* \approx \theta^{**}$
$3\pi/16$	0.07	1.10	0.021	2.32	−0.63	$\theta_0 \approx 1.83$
$\pi/4$	0.096	1.25	0.007	2.5	−0.62	$\theta_0 \approx 2.09$
$5\pi/16$	0.116	1.45	0.003	2.7	−0.69	$\theta_0 \approx 2.35$
$3\pi/8$	0.125	1.60	<0.0005	0.30 and 2.85	−0.71	$\theta_0 \approx 0.53$
$7\pi/16$	0.12	1.72	0.0025	0.45	−0.70	$\theta_0 \approx 0.78$; $\underline{\theta}^{**} \approx 0.9$
$\pi/2$	0.097	1.86	0.0085	0.60	−0.64	$\theta_0 \approx 1.05$; $\underline{\theta}^{**} \approx 1.2$

For this case

$$\frac{\Delta K_{\mathrm{I}}}{\beta K_{\mathrm{I}}^{0}} = 6\int_{\theta^*}^{\theta^{**}} \sin(\theta)\cos(2\varphi-2.5\theta)\left(\sqrt{\frac{H^*}{\sin(\theta)}}-\frac{\sin(\theta)|\cos(2\varphi-1.5\theta)|}{2\sqrt{2}}\right)\mathrm{d}\theta$$

$$-6\int_{\theta^{**}}^{\pi} \sin(\theta)\cos(2\varphi-2.5\theta)\left(\sqrt{\frac{H^{**}}{\sin(\theta)}}-\frac{\sin(\theta)|\cos(2\varphi-1.5\theta)|}{2\sqrt{2}}\right)\mathrm{d}\theta. \quad (34)$$

Case (b). $\pi/8 < \varphi < 3\pi/8$. Referring to Fig. 4(b), we have

$$H^* > H^{**} \text{ with } \theta^* < \theta^{**},$$

and for a half-plane

$$\frac{\Delta K_{\mathrm{I}}}{\beta K_{\mathrm{I}}^{0}} = 6\int_{\theta^*}^{\theta^{**}} \sin(\theta)\cos(2\varphi-2.5\theta)\left(\sqrt{\frac{H^*}{\sin(\theta)}}-\frac{\sin(\theta)|\cos(2\varphi-1.5\theta)|}{2\sqrt{2}}\right)\mathrm{d}\theta$$

$$+6\int_{\theta^{**}}^{\pi} \sin(\theta)\cos(2\varphi-2.5\theta)\left(\sqrt{\frac{H^*}{\sin(\theta)}}-2\sqrt{\frac{H^{**}}{\sin(\theta)}}+\frac{\sin(\theta)|\cos(2\varphi-1.5\theta)|}{2\sqrt{2}}\right)\mathrm{d}\theta\,\mathrm{d}r. \quad (35)$$

Case (c). $3\pi/8 \leqslant \varphi \leqslant \pi/2$. We deduce from Fig. 4(c) that

$$H^* > H^{**} \text{ with } \theta^* > \theta^{**}$$

and the induced SIF for a half-plane is given by

$$\frac{\Delta K_{\mathrm{I}}}{\beta K_{\mathrm{I}}^{0}} = -6\int_{\theta^{**}}^{\theta^*} \sin(\theta)\cos(2\varphi-2.5\theta)\left(\sqrt{\frac{H^{**}}{\sin(\theta)}}-\frac{\sin(\theta)|\cos(2\varphi-1.5\theta)|}{2\sqrt{2}}\right)\mathrm{d}\theta$$

$$+6\int_{\theta^*}^{\pi} \sin(\theta)\cos(2\varphi-2.5\theta)\left(\sqrt{\frac{H^*}{\sin(\theta)}}-\frac{\sin(\theta)|\cos(2\varphi-1.5\theta)|}{2\sqrt{2}}\right)\mathrm{d}\theta. \quad (36)$$

Values of ΔK_{I} for each of the deviatoric and shear transformations in a half-plane are given in Tables 1 and 2, respectively. The transformations induced by the steady-state and quasi-static crack tip stress fields considerably reduce the SIF and, therefore, enhance the fracture toughness for all values of the angle φ between the transformation axis and the crack surface. These results will also be derived by the energy method in Section 7.

6. TOUGHENING ASSOCIATED WITH FERROELASTIC SWITCHING

Virkar and Matsumoto (1986) have shown that switching between different ferroelastic phases may also enhance the fracture toughness of some materials. The switching between ferroelastic phases induces a strain that may interact with the deformation field near a crack tip. Therefore, ferroelastic switching between different phases is another possible toughening mechanism for ferroelastic materials.

We assume that the original material is in one of the two ferroelastic states instead of the paraelastic phase assumed above.

6.1. *Deviatoric switching*

We shall distinguish between the following two cases.

6.1.1. *Initial* Σ_- *phase.* If the initial state is in Σ_- phase, then as stipulated in Section 2, the strain η_2 jumps by 4δ,

$$\varepsilon_{11}^* = 2\delta, \quad \varepsilon_{12}^* = \varepsilon_{21}^* = 0, \quad \varepsilon_{22}^* = -2\delta,$$

when $(\sigma_{11}-\sigma_{22})$ reaches the critical value Σ_c. This switching is different from the paraelastic–ferroelastic transformation discussed above in that the strain jump does not occur even when $(\sigma_{11}-\sigma_{22})$ reaches $-\Sigma_c$. Therefore, the contribution of the switching strain to the SIF is twice that of the contribution of the "Σ_+ phase" transformed zone shown in Fig. 3, where θ_0 is the angle between the adjacent boundaries of the "+phase" region and the "−phase" region.

For stationary cracks, the SIF induced by deviatoric switching for a half-plane is given by

$$\frac{\Delta K_{\mathrm{I}}^{(S)}}{\alpha K_{\mathrm{I}}^0} = 6\sqrt{2}\int_{\theta_0}^{\pi} \sin^2(\theta)\sin(2\varphi-2.5\theta)\sin(2\varphi-1.5\theta)\,\mathrm{d}\theta \quad \text{for} \quad 0 \leqslant \varphi \leqslant \pi/8 \tag{37}$$

and

$$\frac{\Delta K_{\mathrm{I}}^{(S)}}{\alpha K_{\mathrm{I}}^0} = 6\sqrt{2}\int_{0}^{\theta_0} \sin^2(\theta)\sin(2\varphi-2.5\theta)\sin(2\varphi-1.5\theta)\,\mathrm{d}\theta \quad \text{for} \quad \pi/8 < \varphi \leqslant \pi/2. \tag{38}$$

The values of $\Delta K_{\mathrm{I}}^{(S)}$ calculated from eqns (37) and (38) are vanishingly small (the absolute value is smaller than 10^{-5}).

For the steady-state and quasi-static cracks, the corresponding formulae for a half-plane are given below. The values of H^*, H^{**}, θ^*, $\underline{\theta}^*$ and θ^{**} are given in Table 1.

Case (a). $0 \leqslant \varphi \leqslant \pi/8$:

$$\frac{\Delta K_{\mathrm{I}}}{\alpha K_{\mathrm{I}}^0} = 12\int_{\theta^*}^{\pi} \sin(\theta)\sin(2\varphi-2.5\theta)\left(\frac{\sqrt{H^*}}{\sqrt{\sin(\theta)}} - \frac{\sin(\theta)|\sin(2\varphi-1.5\theta)|}{\sqrt{2}}\right)\mathrm{d}\theta. \tag{39}$$

Case (b). $\pi/8 < \varphi < 3\pi/8$:

$$\frac{\Delta K_{\mathrm{I}}}{\alpha K_{\mathrm{I}}^0} = 12\int_{\theta^*}^{\theta^*} \sin(\theta)\sin(2\varphi-2.5\theta)\left(\frac{\sqrt{H^*}}{\sqrt{\sin(\theta)}} - \frac{\sin(\theta)|\sin(2\varphi-1.5\theta)|}{\sqrt{2}}\right)\mathrm{d}\theta. \tag{40}$$

Case (c). $3\pi/8 \leqslant \varphi \leqslant \pi/2$:

$$\frac{\Delta K_{\mathrm{I}}}{\alpha K_{\mathrm{I}}^0} = 12\int_{\theta^*}^{\theta^{**}} \sin(\theta)\sin(2\varphi-2.5\theta)\left(\frac{\sqrt{H^*}}{\sqrt{\sin(\theta)}} - \frac{\sin(\theta)|\sin(2\varphi-1.5\theta)|}{\sqrt{2}}\right)\mathrm{d}\theta\,\mathrm{d}r + 12\int_{\theta^{**}}^{\pi} \sin(\theta)\sin(2\varphi-2.5\theta)\left(\sqrt{\frac{H^*}{\sin(\theta)}} - \sqrt{\frac{H^{**}}{\sin(\theta)}}\right)\mathrm{d}\theta\,\mathrm{d}r. \tag{41}$$

The values of ΔK_{I} computed from eqns (39)–(41) are summarized in Table 3.

Table 3. Toughening associated with the deviatoric switching for steady-state and quasi-static crack growth in a half-plane

φ	0	$\pi/16$	$\pi/8$	$3\pi/16$	$\pi/4$	$5\pi/16$	$3\pi/16$	$7\pi/16$	$\pi/2$
$\Delta K_{\mathrm{I}}/[\alpha K_{\mathrm{I}}^0]$ (initial Σ_- phase)	−0.20	−0.06	negative and vanishingly small	−0.12	−0.38	−0.96	−1.92	−2.04	−2.34
$\Delta K_{\mathrm{I}}/[\alpha K_{\mathrm{I}}^0]$ (initial Σ_+ phase)	−2.34	−2.70	−2.82	−2.64	−2.20	−1.52	−0.96	−0.44	−0.20

6.1.2. *Initial* Σ_+ *phase.* The results for this case can be obtained from the results of Sections 5 and 6.1.1. The values of $\Delta K_I(S)$ calculated for the stationary crack are found to be very small (the absolute value is smaller than 10^{-5}). Results for the steady-state quasi-static crack growth are given in Table 3. The sum of contributions to the SIF from the "+phase" and "−phase" regions for deviatoric switching shown in Table 3 equals twice that of the deviatoric transformation listed in Table 1. This is also true for shear switching.

6.2. *Shear switching*

6.2.1. *Initial* Π_- *phase.* For the static case,

$$\frac{\Delta K_I^{(S)}}{\beta K_I^0} = \frac{6}{\sqrt{2}} \int_0^{\theta_0} \sin^2(\theta) \cos(2\varphi - 2.5\theta) \cos(2\varphi - 1.5\theta)\, d\theta \quad \text{for} \quad 0 \leqslant \varphi < 3\pi/8 \tag{42}$$

and

$$\frac{\Delta K_I^{(S)}}{\beta K_I^0} = \frac{6}{\sqrt{2}} \int_{\theta_0}^{\pi} \sin^2(\theta) \cos(2\varphi - 2.5\theta) \cos(2\varphi - 1.5\theta)\, d\theta \quad \text{for} \quad 3\pi/8 \leqslant \varphi \leqslant \pi/2. \tag{43}$$

Similar to the deviatoric switching cases, we find that the values of $\Delta K_I^{(S)}$ calculated from eqns (42) and (43) are extremely small (the absolute value is smaller than 10^{-5}). Therefore, we conclude that the contribution of the stationary transformed zone to the SIF is always null for the ferroelastic switching studied herein.

For the steady-state quasi-static crack growth, we obtain the following for a half-plane. Values of H^*, H^{**}, θ^*, θ^{**} and $\underline{\theta}^*$ are given in Table 2.

Case (a). $0 \leqslant \varphi \leqslant \pi/8$:

$$\frac{\Delta K_I}{\beta K_I^0} = 12 \int_{\theta^*}^{\theta^*} \sin(\theta) \cos(2\varphi - 2.5\theta) \left(\sqrt{\frac{H^*}{\sin(\theta)}} - \frac{\sin(\theta)|\cos(2\varphi - 1.5\theta)|}{2\sqrt{2}} \right) d\theta. \tag{44}$$

Case (b). $\pi/8 < \varphi < 3\pi/8$:

$$\frac{\Delta K_I}{\beta K_I^0} = 12 \int_{\theta^*}^{\theta^{**}} \sin(\theta) \cos(2\varphi - 2.5\theta) \left(\sqrt{\frac{H^*}{\sin(\theta)}} - \frac{\sin(\theta)|\cos(2\varphi - 1.5\theta)|}{2\sqrt{2}} \right) d\theta$$
$$+ 12 \int_{\theta^{**}}^{\pi} \sin(\theta) \cos(2\varphi - 2.5\theta) \left(\sqrt{\frac{H^*}{\sin(\theta)}} - \sqrt{\frac{H^{**}}{\sin(\theta)}} \right) d\theta\, dr. \tag{45}$$

Case (c). $3\pi/8 \leqslant \varphi \leqslant \pi/2$:

$$\frac{\Delta K_I}{\beta K_I^0} = 12 \int_{\theta^*}^{\pi} \sin(\theta) \cos(2\varphi - 2.5\theta) \left(\sqrt{\frac{H^*}{\sin(\theta)}} - \frac{\sin(\theta)|\cos(2\varphi - 1.5\theta)|}{2\sqrt{2}} \right) d\theta. \tag{46}$$

The values of ΔK_I for shear switching in steady-state crack growth are summarized in Table 4.

Table 4. Toughening associated with the shear switching for steady-state and quasi-static crack growth in a half-plane

φ	0	$\pi/16$	$\pi/8$	$3\pi/16$	$\pi/4$	$5\pi/16$	$3\pi/8$	$7\pi/16$	$\pi/2$
$\Delta K_I/[\beta K_I^0]$ (initial Π_- phase)	−0.18	−0.46	−1.00	−1.02	−1.16	−1.34	−1.42	−1.34	−1.10
$\Delta K_I/[\beta K_I^0]$ (initial Π_+ phase)	−1.10	−0.80	−0.50	−0.24	−0.08	−0.04	negative and vanishingly small	−0.04	−0.18

6.2.2. *Initial* Π_{-}*phase*. The values of ΔK_{I} (S) calculated for the stationary crack are very small (the absolute value is smaller than 10^{-5}); the results for the steady-state crack growth are collected in Table 4. The sum of contributions to the SIF from the "+phase" and "−phase" regions is found to be twice that made by the shear transformation listed in Table 2.

In summary, we conclude that the contribution of the stationary transformed zone to the SIF is always negligible for switching between different ferroelastic phases. However, for the steady-state and quasi-static crack growth, the toughening effects depend strongly on the angle between the principal axis of the transformed material and the crack surface. For all values of this angle discussed herein, both the deviatoric and shear switching reduce the SIF and hence enhance the fracture toughness.

7. ENERGY METHOD FOR STEADY-STATE CRACK GROWTH

The energy method for the calculation of transformation toughening in steady-state and quasi-static crack growth has been developed by, among others, Budiansky *et al.* (1983) and Rose (1987). We now show that the results in Tables 1 and 2 can also be obtained by this method. Using a path-independent integral, Budiansky *et al.* (1983) have derived the following relation for the steady-state quasi-static crack growth in an isotropic elastic material:

$$-2\int_0^H U(y)\,\mathrm{d}y = \frac{2K_{\mathrm{I}}^0\Delta K_{\mathrm{I}}+(\Delta K_{\mathrm{I}})^2}{E}(1-\nu^2), \tag{47}$$

where ΔK_{I} is the SIF induced by the phase transformation near the crack tip, U the strain energy density which depends on the deformation history, H the half-height of the transformed wake and E Young's modulus. For the dilatant transformation, it is found that

$$\int_0^H U(y)\,\mathrm{d}y = H\sigma_m^c\theta^T,$$

where σ_m^c is the critical mean stress for the dilatant transformation and θ^T the transformation dilatation. Ferroelastic switching will occur when a material point shifts from one ferroelastic phase to another ferroelastic phase during the process of steady-state crack growth. We discuss below the deviatoric and shear transformations.

7.1. *Deviatoric transformations*

When $0 \leqslant \varphi < 3\pi/8$, recalling Figs 3(a,b), we obtain

$$\frac{-2\sqrt{2}}{\left(\dfrac{K_{\mathrm{I}}^{0^2}}{\pi\Sigma_c^2}\right)}[H^{**}+2H^{*}] = \frac{\Delta K_{\mathrm{I}}}{\alpha K_{\mathrm{I}}^0} \tag{48}$$

for a half-plane, where we have neglected the second-order term $(\Delta K_{\mathrm{I}})^2$ because the assumption that the effect of transformation-induced stress on the transformed zone is negligible implies that the higher-order effect can be omitted. This is quite reasonable for small transformation zones.

It may be verified that the numerical values of ΔK_{I} given in Table 1 for $0 \leqslant \varphi \leqslant 3\pi/8$ differ from those obtained from eqn (48) by less than 1%. Similarly, for $3\pi/8 \leqslant \varphi \leqslant \pi/2$, we have

$$\frac{-2\sqrt{2}}{\left(\frac{K_I^{0^2}}{\pi\Sigma_c^2}\right)}[H^*+2H^{**}] = \frac{\Delta K_I}{\alpha K_I^0} \tag{49}$$

for a half-plane, which also gives results that agree with those given in Table 1.

7.2. *Shear transformations*

For $0 \leqslant \varphi \leqslant \pi/8$, we have

$$\frac{-4\sqrt{2}}{\left(\frac{K_I^{0^2}}{\pi\Pi_c^2}\right)}[H^{**}+2H^*] = \frac{\Delta K_I}{\beta K_I^0} \tag{50}$$

and for $\pi/8 < \varphi \leqslant \pi/2$

$$\frac{-4\sqrt{2}}{\left(\frac{K_I^{0^2}}{\pi\Pi_c^2}\right)}[H^*+2H^{**}] = \frac{\Delta K_I}{\beta K_I^0} \tag{51}$$

for a half-plane. The numerical values of ΔK_I given in Table 2 differ from those given by eqns (50) and (51) by less than 1.6%. Since we have neglected the influence of the induced stress on the transformed zone, we cannot discuss the so-called "lock-up" phenomenon [see e.g. Rose (1986), Amazigo and Budiansky (1988), Stump and Budiansky (1989) and Andreasen and Karihaloo (1994)]. Due to the lack of experimental data for transformation stresses Σ_c and Π_c, we are unable to discuss quantitatively the toughening effect and compare them with the known "lock-up" condition which defines the limit of validity of the present method. We note that the calculation of toughening effects for steady-state and quasi-static crack growth by the energy method is straightforward. An advantage of the energy method over the method of Sections 5 and 6 is that it may be easily extended to the steady-state crack growth in anisotropic media.

8. CONCLUSIONS

We have evaluated the SIFs induced by the phase transformations near a crack tip in ferroelastic materials whose paraelastic phases are of low anisotropy and have modeled them as isotropic. We have neglected the effects of the transformation-induced stress on the size of the transformed zone. It is found that the stationary transformed zone ahead of a crack tip contributes nothing to the SIF for single and bi-crystals. However, the transformed wake left behind the steady-state quasi-static crack tip always reduces the SIF considerably and therefore enhances the fracture toughness. Similar results for ferroelastic transformations in steady-state and quasi-static crack growth are obtained by the energy method. The toughening effect is found to be insensitive to the angle φ between the principal axis of the transformed material and the crack surface for ferroelastic transformations discussed herein; however, it is very sensitive to this angle for the ferroelastic switching discussed in Section 6. The computed results show that deviatoric and shear transformations and switching induced by the crack tip stress fields enhance the fracture toughness of ferroelastic crystals of low anisotropy. These results are in qualitative agreement with the observations for NiTi-SMA of low anisotropy.

REFERENCES

Achenbach, M. and Muller, I. (1985). Shape memory as a thermally activated process. In *Plasticity Today* (Edited by A. Sawczuk and G. Bianchi), Elsevier Applied Science, London. pp. 515–531.

Aizu, K. (1969). Possible species of "ferroelastic" crystals and of simultaneously ferroelectric and ferroelastic crystals. *J. Phys. Soc. Japan* **27,** 387–396.

Amazigo, J. C. and Budiansky, B. (1988). Steady-state crack growth in supercritically transforming materials. *Int. J. Solids Structures* **24,** 751–755.

Andreasen, J. H. and Karihaloo, B. L. (1994). Surface cracks in transformation toughening ceramics. *Int. J. Solids Structures* **31,** 51–64.

Antolovich, S. D. and Singh, B. (1971). On the toughness increment associated with the austenitic to martensitic phase transformation in TRIP steels. *Met. Trans.* **2,** 2135–2141.

Barsch, G. R. and Krumhansl, J. A. (1988). Nonlinear and nonlocal continuum model of transformation precursors in martensitics. *Met. Trans.* **19A,** 761–775.

Budiansky, B., Hutchinson, J. W. and Lambropoulos, J. C. (1983). Continuum theory of dilatant transformation toughening in ceramics. *Int. J. Solids Structures* **19,** 337–355.

Budiansky, B. and Truskinovsky, L. (1993). On the mechanics of stress-induced phase transformation in zirconia. *J. Mech. Phys. Solids* **41,** 1445–1459.

Delaey, L. and Chandrasekaran, M. (Eds) (1982). Proceedings of the International Conference on Martensitic Transformations (ICOMAT 1982). *J. Phys. Colloq.* **C4.**

Evans, A. G. (1989). The new high-toughness ceramics. In *Fracture Mechanics: Perspectives and Directions, 20th Symp. ASTM STP* **1020** (Edited by R. P. Wei and R. P. Gangloff), pp. 267–291. ASTM Philadelphia.

Falk, F. (1980). Model free energy, mechanics, and thermodynamics of shape memory alloys. *Acta Metall.* **28,** 1773–1780.

Fatuzzo, E. and Merz, W. J. (1967). *Ferroelectricity*. North-Holland, Amsterdam.

Freiman, S. W. (1986). Mechanical properties of ferroelectric ceramics. *IEEE Proc. 6th Int. Symp. on Applications of Ferroelectrics*, Lehigh University, pp. 367–373.

Gao, H. (1989). Applications of 3-D weight functions—I. Formulations of crack interaction with transformation strains and dislocations. *J. Mech. Phys. Solids* **37,** 133–153.

Garvie, R. C., Hannink, R. H. and Pascoe, R. T. (1975). Ceramic steel? *Nature (London)* **258,** 703–704.

Gerberich, W. W., Hemmings, P. L., Zackay, V. F. and Parker, E. R. (1969). Interactions between crack growth and strain-induced transformation. In *Fracture* (Edited by P. L. Pratt), pp. 288–305. Chapman & Hall, London.

Green, D. J., Hannink, R. H. J. and Swain, M. V. (1989). *Transformation Toughening of Ceramics*. CRC Press, Boca Raton, FL.

Hutchinson, J. W. (1974). On steady quasi-static crack growth. Harvard University Report, DEAPS-8 (April 1974).

Jacobs, A. E. (1985). Solitons of the square-rectangular martensitic transformation. *Phys. Rev.* **B31,** 5984–5989.

Jacobs, A. E. (1992). Finite-strain solitons of a ferroelastic transformation in two-dimensions. *Phys. Rev.* **B46,** 8080–8088.

Karihaloo, B. L. and Huang, X. (1989). Three-dimensional elastic crack tip interaction with shear transformation strain. *Int. J. Solids Structures* **25,** 591–607.

Lambropoulos, J. C. (1986). Shear, shape and orientation effects in transformation toughening. *Int. J. Solids Structures* **23,** 1083–1106.

McMeeking, R. M. and Evans, A. G. (1982). Mechanism of transformation toughening in brittle materials. *J. Am. Ceram. Soc.* **65,** 242–246.

Melton, K. N. and Mercier, O. (1981). The mechanical properties of NiTi-based shape memory alloys. *Acta Metall.* **29,** 393–398.

Miyazaki, S., Kawai, T. and Otsuka, K. (1982). Study of fracture in Cu–Al–Ni shape memory bicrystals. *J. Phys. Colloq.* **C4,** 813–818.

Mukunthan, K. and Brown, L. C. (1988). Preparation and properties of fine grain CuAlNi shape memory alloys. *Metall Trans.* **19A,** 2921–2929.

Pohanka, R. C., Freiman, S. W. and Bender, B. A. (1978). Effects of the phase transformation on the fracture behavior of $BaTiO_3$. *J. Am. Ceram. Soc.* **61,** 72–75.

Rose, L. R. F. (1986). The size of the transformed zone during steady-state cracking in transformation toughening materials. *J. Mech. Phys. Solids* **34,** 609–616.

Rose, L. R. F. (1987). The mechanics of transformation toughening. *Proc. R. Soc. Lond.* **A412,** 169–197.

Stump, D. M. (1989). The role of shear strain and shear stress in transformation toughening. *Phil. Mag.* **64,** 879–902.

Stump, D. M. and Budiansky, B. (1989). Crack growth resistance in transformation toughened ceramics. *Int. J. Solids Structures* **25,** 635–646.

Virkar, A. V. and Matsumoto, R. L. K. (1986). Ferroelastic domain switching as a toughening mechanism in tetragonal zirconia. *J. Am. Ceram. Soc.* **69,** c-224–c-226.